

# Designing a parallel manipulator for a specific workspace

J-P. Merlet

INRIA Sophia-Antipolis

**Abstract:** We present an algorithm to determine all the possible geometries of Gough-type 6 d.o.f. parallel manipulators whose workspace has to include a desired workspace. This desired workspace is described as a set of geometric objects, limited here to points and segments, which describe the desired locations of the center of the moving platform. It is assumed that the orientation of the platform is fixed for each given object. This algorithm takes into account the leg length limits, the mechanical limits on the passive joints and interference between links.

## 1 Introduction

In this paper we consider a 6 d.o.f. Gough-type parallel manipulator constituted by a fixed base plate and a mobile plate connected by 6 extensible links (figure 1). For a parallel manipulator, workspace limits are

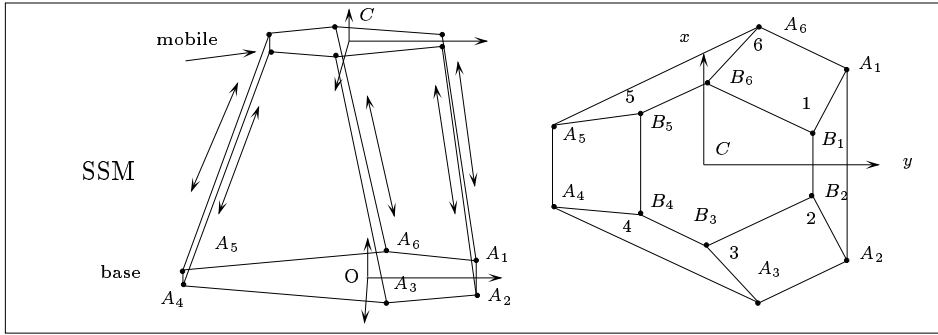


Figure 1: A parallel manipulator

due to the bounded range of linear actuators, mechanical limits on passive joints and interference between links. One important step in the design of a parallel manipulator is to define its geometry according to the desired workspace.

Various geometrical algorithms for computing the workspace boundary when the platform's orientation is kept constant, either in 2D or 3D, have been described by Gosselin (Gosselin 1990; Gosselin, Lavoie, Toutant 1992) when only the constraints on the leg length limits are considered and in (Merlet 1994) when mechanical limits on the joints and interference between the links are also taken into account.

The problem we address in this paper is to find all the possible locations of the centers of the passive joints (point  $A_i$ ,  $B_i$  of figure 1) such that the robot workspace includes the desired workspace. *Note that the proposed algorithms have been implemented in C on a workstation under the X-windows system and every drawings appearing in this paper is a result of this program.*<sup>1</sup>

This research area has been addressed by very few authors. Claudinon (Claudinon, Lievre 1985) has used a numerical method to find the geometry of the robot which optimize some of its kinematics and dynamic features. Stoughton (Stoughton, Kokkinis 1987) has proposed a numerical method for optimizing the workspace of a specific parallel manipulator whose length limits are known. Liu (Liu, Fitzgerald, Lewis 1991; Liu, Fitzgerald, Lewis 1993) has characterized some extremal positions of the robot as a function of its geometry and maximal link lengths. Gosselin (Gosselin, Angeles 1988) has established design rules for the spherical 3 d.o.f parallel manipulator type for obtaining a manipulator enable to perform any kind of rotation. The same author has studied the optimization of the workspace of planar three d.o.f parallel manipulator (Gosselin 1988).

<sup>1</sup>this program is available via anonymous ftp on zenon.inria.fr

Let  $A_i, B_i$  denote the attachment points of the link on the base and on the platform (figure 2). For a pair of  $A_i, B_i$  we attach a reference frame  $O, x, y, z$  to the base such that the  $z$  coordinate of  $A_i$  is equal to 0. In the same manner we attach to the platform a mobile frame  $C, x_r, y_r, z_r$  such that the  $z_r$  coordinate of  $B_i$  is equal to 0. A subscript  $r$  will denote a point or a vector whose coordinates are written in the mobile frame. Let  $\alpha_i$  be the angle between the  $Ox$  axis and  $OA_i$  and let  $\beta_i$  be the angle between the  $Cx_r$  axis and  $CB_{i,r}$ . We denote by  $R_1$  the distance between  $O, A_i$  and  $r_1$  the distance between  $C, B_i$ .

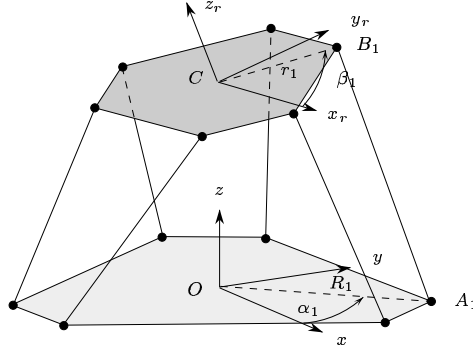


Figure 2: The design parameters for a set of points  $A_i, B_i$  are the distances  $R_1, r_1$  between the points and the origins  $O, C$  of the frames.

Consequently we have:

$$\mathbf{A}_i \mathbf{O} = \begin{pmatrix} -R_1 \cos \alpha_i \\ -R_1 \sin \alpha_i \\ 0 \end{pmatrix} = R_1 \mathbf{u}_i \quad \mathbf{CB}_{i,r} = \begin{pmatrix} r_1 \cos \beta_i \\ r_1 \sin \beta_i \\ 0 \end{pmatrix} = r_1 \mathbf{v}_i \quad (1)$$

where  $\mathbf{u}_i, \mathbf{v}_i$  are unit vectors. As soon as the values of  $R_1, r_1$  are fixed for each pair of  $(A_i, B_i)$  the geometry of the robot is completely determined. The purpose of this paper is to determine all the possible values of  $R_1, r_1$  for each pair of  $(A_i, B_i)$  such that the workspace of the corresponding robot includes a given workspace under the following assumptions:

- the minimum and maximum value of the leg lengths are known.
- the angles  $\alpha_i, \beta_i$  are known.

For that purpose we attach a plane  $\mathcal{P}_i$  to each pair of  $A_i, B_i$ , with a frame whose axis will correspond to the value of the  $R_1, r_1$  parameters for the pair  $A_i, B_i$ . The algorithm presented in the sequel will compute the boundary of the regions of this plane such that any point in the regions defines a robot whose workspace includes the specified workspace. The regions will therefore be called the *allowable region* for the pair  $(A_i, B_i)$ .

As for the desired workspace we will assume that it is defined as a set of geometric objects such as points, segments, planar polygons... describing the location of the point  $C$  of the moving platform, the orientation of the moving platform being fixed for each object. In this paper we will examine the case where the desired workspace is specified in term of points and segments workspace although possible extensions will be mentioned.

## 2 Points workspace

In the following sections we will assume that the desired workspace  $W$  is specified by a set of  $n$  pairs of elements:

$$W = \{(H_i, Rot_i), i \in [1, n]\}$$

where  $H_i$  is the desired location of  $C$  and  $Rot_i$  is a rotation matrix defining the orientation of the moving platform at  $H_i$ .

## 2.1 Allowable regions for the length constraints

In this section we will assume that the constraints limiting the workspace are only the leg lengths. The minimum and maximum values of these lengths will be denoted by  $\rho_{min_i}, \rho_{max_i}$ . The position of the robot is defined by the coordinates of  $C$  in the fixed frame and the rotation matrix  $Rot$  between the fixed and mobile frames.

Assume that only one leg has length constraints. The corresponding pair  $(A_i, B_i)$  will now be denoted  $(A, B)$ . For a given posture of the moving platform defined by a pair  $(H, Rot)$  the leg length  $\rho$  is the norm of the vector  $\mathbf{AB}$ . We have:

$$\rho^2 = \|\mathbf{AB}\|^2 = \mathbf{AO} \cdot \mathbf{AO}^T + \mathbf{HB} \cdot \mathbf{HB}^T + 2(\mathbf{AO} + Rot \mathbf{HB}_r) \cdot \mathbf{OH}^T + 2R\mathbf{HB}_r \cdot \mathbf{AO}^T + \mathbf{OH} \cdot \mathbf{OH}^T \quad (2)$$

This equation may be rewritten as:

$$\rho^2 = R_1^2 + r_1^2 + R_1 r_1 Rot \mathbf{v} \cdot \mathbf{u}^T + R_1 \mathbf{u} \cdot \mathbf{OH}^T + r_1 Rot \mathbf{v} \cdot \mathbf{OH}^T + \mathbf{OH} \cdot \mathbf{OH}^T \quad (3)$$

We define  $\mathcal{E}(H, \rho)$  as:

$$R_1^2 + r_1^2 + R_1 r_1 Rot \mathbf{v} \cdot \mathbf{u}^T + R_1 \mathbf{u} \cdot \mathbf{OH}^T + r_1 Rot \mathbf{v} \cdot \mathbf{OH}^T + \mathbf{OH} \cdot \mathbf{OH}^T - \rho^2 = 0 \quad (4)$$

For a given  $\rho$  equation (4) defines an ellipse in the  $R_1 - r_1$  plane, the plane  $\mathcal{P}$  attached to the pair  $(A, B)$ . It is then easy to prove the following theorem:

**Theorem 1** *Let  $M$  be a point in the  $R_1, r_1$  plane. If we have  $\mathcal{E} \leq 0$  (i.e.  $M$  is inside the ellipse), then the length of the leg is less than or equal to  $\rho$  for the corresponding posture  $(H, R)$ .*

We define the *maximal ellipse* for  $(H_i, Rot_i)$  as  $\mathcal{E}(H_i, \rho_{max})$ . For any point  $M$  in the  $R_1, r_1$  plane such that  $\mathcal{E}(H_i, \rho_{max}) \leq 0$  (i.e.  $M$  is inside the maximal ellipse), then the leg length is less than or equal to  $\rho_{max}$ . For any  $M$  outside the maximal ellipse the leg length is greater than  $\rho_{max}$ . Consequently this ellipse defines the allowable region for the maximum length constraint.

We may also define the *minimal ellipse* for  $(H_i, Rot_i)$  as  $\mathcal{E}(H_i, \rho_{min})$ . For any point  $M$  in the  $\mathcal{P}$  plane outside the ellipse (i.e.  $\mathcal{E}(H_i, \rho_{min}) > 0$ ), then the length leg is greater than  $\rho_{min}$ . Consequently the minimal ellipse defines the values of the pair  $R_1, r_1$  such that the minimum length constraint are violated: this region of  $\mathcal{P}$  is forbidden.

It is easy now to determine the allowable region for the pair  $(A, B)$  and the set of postures  $(H_i, Rot_i)$  in the  $R_1, r_1$  plane. Indeed for each posture  $(H_i, Rot_i)$  of the moving platform the points of the allowable region must be inside every maximal ellipses and outside every minimal ellipses. Consequently any point of the allowable region belongs to the *intersection* of the maximal ellipses and does not belong to the *union* of the minimal ellipses. In other words the allowable region  $\mathcal{A}_l$  may be computed as:

$$\mathcal{A}_l = \cap_{i=1}^{i=n} \mathcal{E}(H_i, \rho_{max}) - \cup_{i=1}^{i=n} \mathcal{E}(H_i, \rho_{min})$$

$\mathcal{A}_l$  is computed by using the following algorithm:

1. for each posture  $H_i, Rot_i$  compute the maximal ellipse
2. compute the intersection  $\mathcal{I}_{H, Rot}$  of all the maximal ellipses
3. for each posture  $H_i, Rot_i$  compute the minimal ellipse
4. compute the union  $\mathcal{U}_{H, Rot}$  of all the minimal ellipses
5. compute  $\mathcal{A}_l$  as  $\mathcal{I}_{H, Rot}$  minus  $\mathcal{U}_{H, Rot}$

A special case should be mentioned: if all the attachment points  $A_i, B_i$  lie on circles, then the planes  $\mathcal{P}_i$  attached to the pairs  $(A_i, B_i)$  are identical and there are now only two design parameters, the two values of the circle radii. The intersection of the allowable regions  $\mathcal{A}_l^i$  obtained for each pair  $(A_i, B_i)$  will define the allowable region i.e. the possible values of the circle radii.

## 2.2 Allowable region for the mechanical limits on the joints

Not all rotation may be performed by a real ball-and-socket joint but its mechanical limits may be taken into account in the design process.

### 2.2.1 A model for the mechanical limits

We have introduced in (Merlet 1994) a model for the mechanical limits on the passive joints. These limits are defined by the user as a pyramid whose apex is the joint center and whose faces are such that if the joint constraints are satisfied, then the link will be inside the interior of the pyramid. For the joints attached to the base the apex of this pyramid is located at point  $A_i$  (Figure 3).

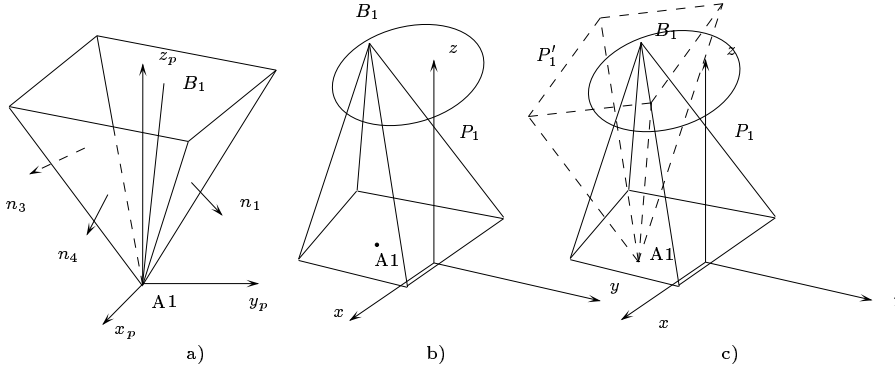


Figure 3: Example of model for the constraints on a passive joint located at  $A_1, B_1$ . In a) if the mechanical limits of the joint at  $A_1$  are satisfied, then link  $A_1B_1$  is inside the volume delimited by the pyramid. Frame  $A_1(x_p, y_p, z_p)$  is a fixed frame. In b)  $P_1$  is the pyramid for the joint at  $B_1$  from which we deduce (c) the equivalent pyramid  $P'_1$  whose apex is located in  $A_1$ .

For the passive joints attached to the moving platform we may use the same model. Indeed we may define a pyramid  $P_i$  with apex  $B_i$  such that if the constraint on the joint at  $B_i$  are satisfied, then point  $A_i$  lie inside the pyramid. From this pyramid we deduce an *equivalent pyramid*  $P'_i$  to  $P_i$ , whose apex is  $A_i$ , such that if  $A_i$  lie inside  $P'_i$ , then  $B_i$  lie inside  $P_i$  (figure 3).

### 2.2.2 Allowable region

Let  $\mathbf{n}_j^i, j \in [1, k]$  denote the normals to the  $k$  faces of the pyramid for a joint of leg  $i$ . For a given posture of the moving platform the link  $A_iB_i$  lie inside the pyramid (meaning that the joint lie within its mechanical limits) if:

$$\mathbf{A}_i\mathbf{B}_i \cdot \mathbf{n}_j^i \leq 0 \quad \forall j \in [1, k]$$

For a pair  $(A, B)$  and a given normal  $\mathbf{n}$  the previous inequality may be rewritten as:

$$R_1 \mathbf{u} \cdot \mathbf{n}^T + r_1 R \mathbf{v} \cdot \mathbf{n}^T + \mathbf{O} \mathbf{H}_i \cdot \mathbf{n}^T \leq 0 \quad (5)$$

We define  $\mathcal{L}(R_1, r_1, H_i)$  as the left side of this inequality. The equation  $\mathcal{L}(R_1, r_1, H_i) = 0$  defines a line in the  $\mathcal{P}$  plane. This line separates the plane in two half-planes  $\mathcal{P}_{-1}, \mathcal{P}_{+1}$  with  $\mathcal{L}(R_1, r_1, H_i) \leq 0$  if  $(R_1, r_1)$  belongs to  $\mathcal{P}_{-1}$  and  $\mathcal{L}(R_1, r_1, H_i) > 0$  if  $(R_1, r_1)$  belongs to  $\mathcal{P}_{+1}$ . Therefore the half-plane  $\mathcal{P}_{-1}$  is the allowable region for the joint and for this face of the pyramid. To determine the allowable region  $\mathcal{A}_p^i$  for the joint  $i$  for a given posture of the moving platform we compute the allowable half-plane for each normal, then we compute the intersection of all these half-planes.

The allowable region  $\mathcal{A}_p$  for a set of postures  $(H_i, Rot_i)$  is simply the intersection of the allowable regions  $\mathcal{A}_p^i$  obtained for each posture.

## 2.3 Allowable region for links interference

### 2.3.1 Principle of the computation of the allowable region

In this section we will assume that the links have no thickness and furthermore that all the attachment points lie on circles (i.e. the  $R_1, r_1$  parameters are shared by all the attachment points). Our purpose is to determine the values of  $R_1, r_1$  for which there is no interference between any pair of links. Without loss of generality we will consider legs 1 and 2. The links will interfere if:

- the associated lines interfere
- the common perpendicular to the line has points belonging to both links  $A_1B_1, A_2B_2$

If the two lines intersect then:

$$\mathbf{A}_1\mathbf{A}_2 \cdot (\mathbf{A}_1\mathbf{B}_1 \times \mathbf{A}_2\mathbf{B}_2)^T = 0 \quad (6)$$

which may be written as:

$$-R_1r_1(b_1R_1 + b_2r_1 + b_3) = 0 \quad (7)$$

with the  $b_i$ 's defined by:

$$\begin{aligned} b_1 &= (\mathbf{u}_2 - \mathbf{u}_1) \cdot (\text{Rot } \mathbf{v}_2 \times \mathbf{u}_1 + \mathbf{u}_2 \times \text{Rot } \mathbf{v}_1)^T \\ b_2 &= (\mathbf{u}_2 - \mathbf{u}_1) \cdot (\text{Rot } \mathbf{v}_1 \times \text{Rot } \mathbf{v}_2)^T \\ b_3 &= (\mathbf{u}_2 - \mathbf{u}_1) \cdot (\mathbf{OH} \times \text{Rot } \mathbf{v}_2 + \text{Rot } \mathbf{v}_1 \times \mathbf{OH})^T \end{aligned}$$

which are therefore constants defined by the geometry and the posture of the platform. As we may assume that  $R_1 \neq 0$  and  $r_1 \neq 0$  various cases can be considered:

- if  $b_1 = b_2 = b_3 = 0$  the lines intersect whatever are the dimensions of the robot
- if  $b_1 = b_2 = 0, b_3 \neq 0$  the lines will never intersect
- otherwise the lines intersect if the  $R_1, r_1$  are on a line in the  $\mathcal{P}$  plane.

Hence in each case we can define a variety  $\mathcal{V}$  of  $\mathcal{P}$  for which the lines intersect:  $\mathcal{P}$  itself for the first case, the empty set for the second case and a line for the last case. Now we have to express that the intersection point of the lines belongs to both links. We project the points  $A_1, A_2, B_1, B_2$  onto the plane  $O, x, y$  of the reference frame and denote by a superscript  $P$  the projected points. If the segments  $A_1B_1, A_2B_2$  intersect, then their projections will also intersect and the intersection point of the lines will belong to the link in two cases. The first one is obtained when:

$$(\mathbf{A}_1\mathbf{B}_1^P \times \mathbf{B}_1\mathbf{B}_2^P)_z \geq 0 \quad (\mathbf{B}_2\mathbf{A}_2^P \times \mathbf{B}_2\mathbf{B}_1^P)_z \leq 0 \quad (8)$$

$$(\mathbf{A}_1\mathbf{A}_2^P \times \mathbf{A}_1\mathbf{B}_1^P)_z \leq 0 \quad (\mathbf{A}_2\mathbf{A}_1^P \times \mathbf{A}_2\mathbf{B}_2^P)_z \geq 0 \quad (9)$$

where the subscript  $_z$  denotes the  $z$  component of the vector. The second case is obtained when:

$$(\mathbf{A}_1\mathbf{B}_1^P \times \mathbf{B}_1\mathbf{B}_2^P)_z < 0 \quad (\mathbf{B}_2\mathbf{A}_2^P \times \mathbf{B}_2\mathbf{B}_1^P)_z > 0 \quad (10)$$

$$(\mathbf{A}_1\mathbf{A}_2^P \times \mathbf{A}_1\mathbf{B}_1^P)_z > 0 \quad (\mathbf{A}_2\mathbf{A}_1^P \times \mathbf{A}_2\mathbf{B}_2^P)_z < 0 \quad (11)$$

The quantities which appear on the left side of the inequalities may be expressed as function of  $R_1, r_1$ . They have all the same generic form:

$$R_1(e_1R_1 + e_2r_1 + e_3) \quad \text{or} \quad r_1(e_1R_1 + e_2r_1 + e_3)$$

Each inequality will therefore be verified if  $R_1, r_1$  belongs to a region of  $\mathcal{P}$  obtained as the intersection of a half-plane bounded by  $e_1R_1 + e_2r_1 + e_3 = 0$  and one of the half-plane defined by the sign of  $R_1$  or  $r_1$ . For each set of inequalities we first compute the intersection of the four regions. Then we intersect the result with the variety  $\mathcal{V}$  defined by equation (7). The resulting region  $\mathcal{F}_i^{12}$  of  $\mathcal{P}$  defines all the robots for which leg interference occurs. This region may be either a region, a line, a segment, a point or the empty set. This process is repeated for each pair of links and for each posture of the desired workspace. The forbidden region for links interference is then the union of all the  $\mathcal{F}_i^{jk}$ .

### 3 Segments workspace

In the following sections the desired workspace is described by a set of pairs (segment, orientation). For each pair point  $C$  should be able to describe the segment while the moving platform has the orientation defined in the pair.

#### 3.1 Allowable regions for the length constraints

##### 3.1.1 Sets of maximal and minimal ellipses

In this section we will assume that the constraints limiting the workspace are only the leg lengths. A trajectory segment is defined by two points  $M_1(x_1, y_1, z_1)$ ,  $M_2(x_2, y_2, z_2)$  and for any  $C$  belonging to the trajectory we may write:

$$\mathbf{OC} = \mathbf{OM}_1 + \lambda \mathbf{M}_1 \mathbf{M}_2 \quad (12)$$

where  $\lambda$  is a scalar parameter in the range  $[0,1]$ . Remember that the leg length  $\rho$  is the norm of the vector  $\mathbf{AB}$ . For a point  $C$  on the segment we have:

$$\rho^2 = \|\mathbf{AB}\|^2 = \mathbf{AO} \cdot \mathbf{AO}^T + \mathbf{CB} \cdot \mathbf{CB}^T + 2(\mathbf{AO} + \text{Rot } \mathbf{CB}_r) \cdot \mathbf{OC}^T + 2 \text{Rot } \mathbf{CB}_r \cdot \mathbf{AO}^T + \mathbf{OC} \cdot \mathbf{OC}^T \quad (13)$$

Using equations (1,12) this equation may be rewritten as:

$$\rho^2 = R_1^2 + r_1^2 + R_1 r_1 \text{Rot } \mathbf{v} \cdot \mathbf{u} + R_1 \mathbf{u} \cdot (\mathbf{OM}_1 + \lambda \mathbf{M}_1 \mathbf{M}_2)^T + r_1 \text{Rot } \mathbf{v} \cdot (\mathbf{OM}_1 + \lambda \mathbf{M}_1 \mathbf{M}_2)^T + \lambda^2 \mathbf{M}_1 \mathbf{M}_2 \cdot \mathbf{M}_1 \mathbf{M}_2^T + \mathbf{OM}_1 \cdot \mathbf{OM}_1^T + 2\lambda \mathbf{OM}_1 \cdot \mathbf{M}_1 \mathbf{M}_2^T$$

or in another form:

$$R_1^2 + r_1^2 + a_0 R_1 r_1 + R_1(a_1 \lambda + a_2) + r_1(a_3 \lambda + a_4) + a_5 \lambda^2 + a_6 \lambda + a_7 = 0 \quad (14)$$

$$\mathcal{E}(R_1, r_1, \lambda, \rho) = 0 \quad (15)$$

$$F(\lambda) = A_2 \lambda^2 + A_1 \lambda + A_0 = 0 \quad (16)$$

In equation (14) the  $a_i$  coefficients are only dependent on the known design parameters and on the coordinates of  $M_1, M_2$ . The structure of equation (14) leads to the following theorem:

**Theorem 2** For a given set of  $\rho, \lambda$  equation (14) defines an ellipse in the  $R_1 - r_1$  plane or has no solution in  $R_1, r_1$ .

Consider now the function  $\mathcal{E}_{max}(\lambda) = \mathcal{E}(R_1, r_1, \lambda, \rho_{max})$  with  $\lambda$  in the range  $[0,1]$ . This function defines a set of maximal ellipses. If  $\mathcal{E}(R_1, r_1, \lambda, \rho_{max}) \leq 0$  for any  $\lambda$  in the range  $[0,1]$ , then the leg length is less than or equal to  $\rho_{max}$  for any posture of the moving platform on the trajectory. Consequently the allowable region for the maximum length constraint is the set of points  $M(R_1, r_1)$  such that  $\mathcal{E}_{max}(\lambda) \leq 0$  for any  $\lambda$  in  $[0,1]$ . Hence any such  $M$  point must be inside all the maximal ellipses of the set and therefore the allowable region with respect to the constraint  $\rho \leq \rho_{max}$  is the intersection  $\mathcal{I}$  of all the maximal ellipses. We denote  $\mathcal{E}_{max}(0)$  and  $\mathcal{E}_{max}(1)$  the two ellipses obtained for  $\lambda = 0$  and  $\lambda = 1$ . The following theorems hold:

**Theorem 3** As  $\lambda$  vary the centers of the corresponding maximal ellipses lie on a segment which in some cases may be reduced to a point. The angle between the main axis of the ellipses and the  $R_1$  axis is  $\pi/4$ .

**Theorem 4** If the maximal ellipses  $\mathcal{E}_{max}(0)$ ,  $\mathcal{E}_{max}(1)$  exists, then the ellipse exist for any value of  $\lambda$  in the range  $[0,1]$ .

**Theorem 5** The intersection  $\mathcal{I}$  of all the ellipses in the set is equal to

$$\mathcal{E}_{max}(0) \cap \mathcal{E}_{max}(1)$$

Therefore the allowable region is simply the intersection of the ellipses computed for the extremal points of the trajectory.

Note that the last theorem is a simple consequence of the fact that the workspace corresponding to  $\rho_{max}$  is convex. Indeed this workspace is the intersection of the 6 spheres which are obtained by translating the spheres centered in  $A_i$  with radii  $\rho_{max}^i$  by the fixed vector  $\mathbf{B}_i\mathbf{C}$ . As the result of the intersection of spheres the workspace is convex.

Let  $\mathcal{E}_{min}(\lambda)$  be the function  $\mathcal{E}(R_1, r_1, \lambda, \rho_{min})$ . This function defines a set of minimal ellipses. If  $\mathcal{E}_{min}(\lambda) > 0$  for a given point  $M$  and a given  $\lambda$ , then the corresponding leg length is greater than  $\rho_{min}$ . Therefore for any point belonging to the allowable region this relation has to be verified for all  $\lambda$  in  $[0,1]$ . Consequently any point of the allowable region must lie outside the region  $\mathcal{U}$  defined by the union of the minimal ellipses. Hence the allowable region  $\mathcal{A}_l$  for the leg length constraint is:

$$\mathcal{A}_l = (\mathcal{E}_{max}(0) \cap \mathcal{E}_{max}(1)) - \mathcal{U} \quad (17)$$

### 3.1.2 The "growing" algorithm

The main difficulty for the computation of  $\mathcal{A}_l$  lie in obtaining the region  $\mathcal{U}$ . For this purpose we may use an efficient method, the "growing" algorithm which was first suggested by Troyanov (Troyanov 1995). The constraint which defines the region  $\mathcal{U}$  is  $\|\mathbf{AB}\|^2 \leq \rho_{min}^2$ . The vector  $\mathbf{AB}$  may be written as:

$$\mathbf{AB} = R_1\mathbf{u} + \mathbf{OC} + r_1\mathbf{v} \quad (18)$$

Let  $\Pi$  be the plane defined by point  $O$  and vectors  $\mathbf{u}, \mathbf{v}$ . Let  $M$  be a point of this plane such that  $\mathbf{MO} = R_1\mathbf{u} + r_1\mathbf{v}$ . The forbidden region is the set of points  $M$  such that:

$$\|\mathbf{AB}\|^2 = \|\mathbf{MC}\|^2 \leq \rho_{min}^2 \quad (19)$$

Hence for a fixed  $C$  the forbidden region is the intersection of the plane  $\Pi$  with the sphere of radius  $\rho_{min}$  centered at  $C$ . When  $C$  lies on a segment  $M_1M_2$  the forbidden region is obtained by "growing" the segment by  $\rho_{min}$  i.e. by first constructing the 3D volume, called the "grown" volume, of the points which are at a distance less than or equal to  $\rho_{min}$ , then by intersecting this volume with the plane  $\Pi$ . The "growing" of a segment leads to a portion of cylinder of height  $\|\mathbf{M}_1\mathbf{M}_2\|$  and radius  $\rho_{min}$  topped by two half spheres of radius  $\rho_{min}$  centered at  $M_1, M_2$  (figure 4). In practice the intersection of the

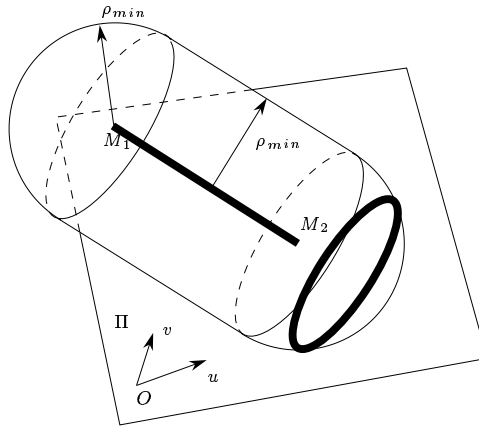


Figure 4: The growing of a segment  $M_1M_2$  by  $\rho_{min}$  leads to a volume composed of a portion of a cylinder topped by two half spheres. The intersection of this volume with the plane  $\Pi$  gives the forbidden region (here the region delimited by the ellipse is in thick lines) in the  $O, \mathbf{u}, \mathbf{v}$  frame.

grown volume and the  $\Pi$  plane is computed in the frame  $O, \mathbf{u}, \mathbf{v}$  and is approximated by a polygon. The coordinates of the vertices of this polygon are then expressed in the frame of the  $\mathcal{P}$  plane, thus leading to a polygonal approximation of the forbidden region.

### 3.1.3 Computation of the allowable region for a set of segments

The computation of the allowable region for the leg length constraints is done using the following algorithm:

1. for each segment trajectory determine the allowable region using the following algorithm:
  - (a) compute the maximal ellipses for the extreme points of the trajectory
  - (b) compute the intersection  $\mathcal{I}$  of these two ellipses. If it is empty there is no allowable region.
  - (c) compute the union  $\mathcal{U}$  of the minimal ellipses using the "growing" algorithm
  - (d) subtract  $\mathcal{U}$  to  $\mathcal{I}$  to get the allowable region for the trajectory
2. compute the intersection of all the allowable regions

In our implementation the boundary of all the regions are approximated by polygons in order to simplify the intersection and the boolean operations on the regions. Figure 5 shows a result of this algorithm, when the desired workspace is defined by one segment. Another example is shown on figure 6: three

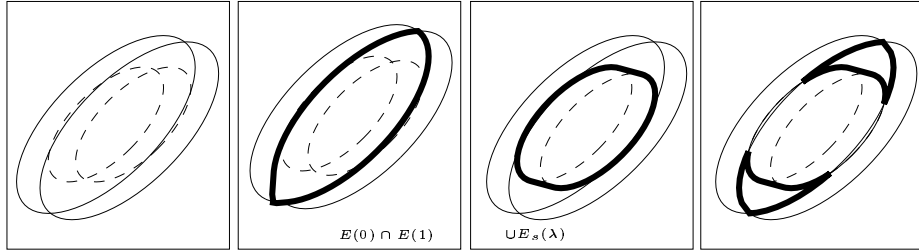


Figure 5: The computation of the allowable region. On the left side are drawn the maximal ellipses for the extreme point of the trajectory (in thin line) and the minimal ellipses for the same points (in dashed line). The intersection of the maximal ellipses is shown on the second drawing. The union of the forbidden ellipses is shown on the third drawing. The boundary of the allowable region is shown in thick line on the last drawing (first segment, trajectory 0, first set of length limits).

segments have been defined and it is assumed that all the attachment points lie on the same circle (the allowable region is therefore the intersection of the allowable regions of each leg). In another example we have defined 64 trajectories with identical start point  $(0,0,50)$  and end points uniformly distributed on the sphere of radius 5 centered at the start point. Figure 7 shows the 3D representation of the workspace of a particular robot defined by a point in the allowable region together with the 64 trajectories (in thick lines).

## 3.2 Allowable region for mechanical limits on the joints

In this section we will use the model for the mechanical limits described in the point workspace. For a given posture of the moving platform the leg  $A_i B_i$  will lie inside the pyramid (which means that the mechanical limits of the joint are not violated) if

$$\mathbf{A}_i \mathbf{B}_i \cdot \mathbf{n}_j^T \leq 0 \quad \forall j \in [1, k]$$

Using equation (12) the previous inequality may be rewritten for a specific leg and a specific face of a pyramid as:

$$R_1 \mathbf{u} \cdot \mathbf{n}^T + r_1 R \mathbf{v} \cdot \mathbf{n}^T + \lambda \mathbf{M}_1 \mathbf{M}_2 \cdot \mathbf{n}^T + \mathbf{O} \mathbf{M}_1 \cdot \mathbf{n}^T \leq 0 \quad (20)$$



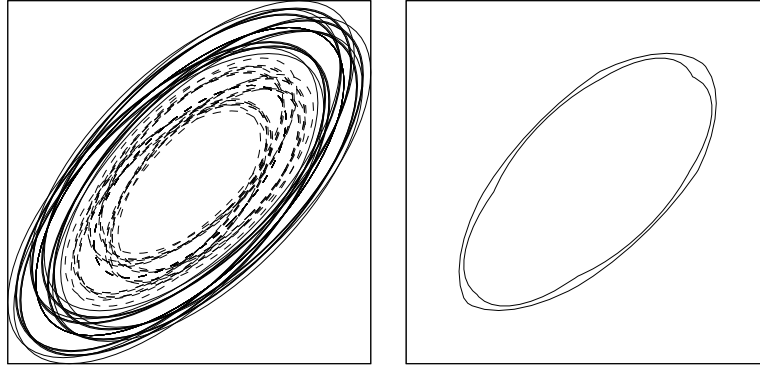


Figure 6: On the left the minimal ellipses (dashed lines) and the maximal ellipses (in thin lines) for a workspace defined by three segments. On the right the allowable region.

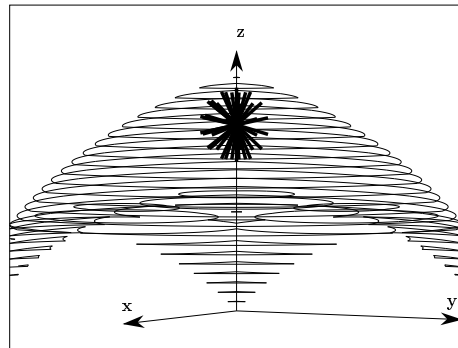


Figure 7: For a given robot defined by a point in the allowable region the 64 trajectories (in thick lines) approximating a sphere are effectively inside the workspace.

Let  $\mathcal{L}(R_1, r_1, \lambda)$  denotes the left side of this inequality. The equation  $\mathcal{L}(R_1, r_1, \lambda) = 0$  defines a set of lines with identical slope in the  $R_1, r_1$  plane which span a region in the plane whose boundary is constituted of the line  $\mathcal{L}(R_1, r_1, 0) = L_0$ ,  $\mathcal{L}(R_1, r_1, 1) = L_1$ . One of the two lines  $L_0, L_1$  separates the plane in two half-planes  $\mathcal{P}_{+1}, \mathcal{P}_{-1}$  such that  $\mathcal{L}(R_1, r_1, \lambda) \leq 0$  for any  $\lambda$  in  $[0,1]$  if  $M(R_1, r_1)$  belongs to  $\mathcal{P}_{-1}$  and  $\mathcal{L}(R_1, r_1, \lambda) > 0$  for some values of  $\lambda$  in  $[0,1]$  if  $M$  belongs to  $\mathcal{P}_{+1}$ . Therefore  $\mathcal{P}_{-1}$  defines a half-plane which is the allowable region for this face of the pyramid.

The process is repeated for each face of the pyramid, leading to a set of half-planes. The intersection of these half-planes is the allowable region with respect to the mechanical limits on the joint. An example of this computation is shown in figure 8.

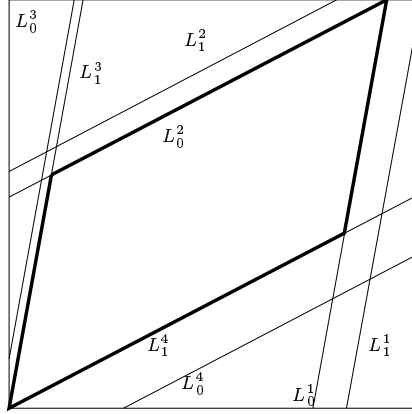


Figure 8: The mechanical limits of this particular joint is described by a four-faced pyramid. We have computed the separating half-plane  $\mathcal{P}_{-1}$  for each of the faces. The intersection of these half-planes define a closed region with the boundary in thick line, which is the allowable region for this joint.

### 3.3 Forbidden region for interference between the links

We will consider interference between links 1 and 2 without loss of generality. If the two lines associated to these links intersect then:

$$\mathbf{A}_1 \mathbf{A}_2 \cdot (\mathbf{A}_1 \mathbf{B}_1 \times \mathbf{A}_2 \mathbf{B}_2)^T = 0 \quad (21)$$

which may be written as:

$$-R_1 r_1 (b_1 \lambda + b_2 R_1 + b_3 r_1 + b_4) = 0 \quad (22)$$

with

$$\begin{aligned} b_1 &= (\mathbf{u}_2 - \mathbf{u}_1) \cdot (\mathbf{M}_1 \mathbf{M}_2 \times \text{Rot } \mathbf{v}_2 + \text{Rot } \mathbf{v}_1 \times \mathbf{M}_1 \mathbf{M}_2)^T \\ b_2 &= (\mathbf{u}_2 - \mathbf{u}_1) \cdot (\text{Rot } \mathbf{v}_2 \times \mathbf{u}_1 + \mathbf{u}_2 \times \text{Rot } \mathbf{v}_1)^T \\ b_3 &= (\mathbf{u}_2 - \mathbf{u}_1) \cdot (\text{Rot } \mathbf{v}_1 \times \text{Rot } \mathbf{v}_2)^T \\ b_4 &= (\mathbf{u}_2 - \mathbf{u}_1) \cdot (\mathbf{O} \mathbf{M}_1 \times \text{Rot } \mathbf{v}_2 + \text{Rot } \mathbf{v}_1 \times \mathbf{O} \mathbf{M}_1)^T \end{aligned}$$

Hence the  $b_i$ 's are constants defined by the known design parameters and the trajectory of the platform. Various cases can now be considered:

1.  $b_1 = b_2 = b_3 = b_4 = 0$ : the lines intersect whatever is the dimension of the robot for any position on the trajectory of the robot.
2.  $b_1 = 0$ : the lines will intersect if the  $R_1, r_1$  are on a line in the  $R_1, r_1$  plane

3. in the general case the lines will intersect if the  $R_1, r_1$  are on a set of lines of  $\mathcal{P}$

Hence in each case we may define a variety  $\mathcal{V}$  of  $\mathcal{P}$  for which the lines intersect:  $\mathcal{P}$  itself for the first case, the empty set for the second case. In the last case  $\mathcal{V}$  is the region delimited by the lines  $b_1 + b_2 R_1 + b_3 r_1 + b_4 = 0$  and  $b_2 R_1 + b_3 r_1 + b_4 = 0$ . Now we can look for the sub-variety  $\mathcal{V}_u$  of  $\mathcal{V}$  for which the the links intersect using the inequalities (8,9), (10,11).

The quantities which appear on the left side of these inequalities may be expressed as function of  $\lambda, R_1, r_1$ . They have all the same generic form:

$$R_1(e_1\lambda + e_2R_1 + e_3r_1 + e_4) \text{ or } r_1(e_1\lambda + e_2R_1 + e_3r_1 + e_4)$$

First it must be noted that these inequalities may define an unbounded variety  $\mathcal{V}_u$ . In order to compute the allowable region we will have to subtract  $\mathcal{V}_u$  from the allowable regions determined using the other constraints.  $\mathcal{V}_u$  is divided in four regions  $Q_i$  defined by:

$$\begin{array}{ll} R_1 \geq 0 & r_1 \geq 0 \\ R_1 \leq 0 & r_1 \leq 0 \end{array} \quad \begin{array}{ll} R_1 \leq 0 & r_1 \leq 0 \\ R_1 \geq 0 & r_1 \leq 0 \end{array}$$

In each region  $Q_i$  the sign of the inequalities is now fully defined by the sign of the second term  $\mathcal{S}$  of the inequalities:

$$\mathcal{S} = e_1^i \lambda + e_2^i R_1 + e_3^i r_1 + e_4^i$$

which define a set of lines. One of these lines split  $Q_i$  into two sub-regions  $Q_{i+1}, Q_{i-1}$ , one of them such that  $\mathcal{S}$  is either positive or negative for any  $\lambda$  in the range  $[0,1]$ . For each  $Q_i$  we retain the sub-regions for which the inequalities (8,9), (10,11) are satisfied and compute their union. The intersection of this union with the variety  $\mathcal{V}$  define the region of  $Q_i$  for which the links intersect. Figure 9 shows an example of such computation. The process is then repeated for each pair of links.

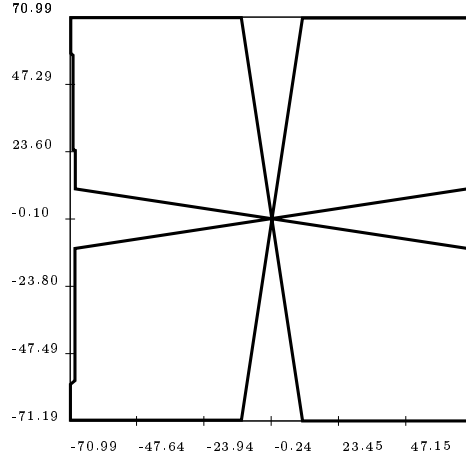


Figure 9: The region in the  $R_1, r_1$  plane for which link 0 will interfere with some other link.

### 3.4 Verifying all the constraints

We may now compute the allowable region for a set of segments using the following steps:

1. for each segment of the set:
  - compute the allowable region for the leg length constraint and mechanical limits constraint

- compute the forbidden region for the leg interference constraint
2. compute the intersection of all allowable regions
  3. compute the union of all forbidden regions
  4. subtract the union to the intersection, the result is the allowable region

Figure 10 shows a result of this algorithm. In this example it is assumed that all the joint centers of the base and the platform lie on the same circles (i.e all the pairs  $(A, B)$  share the same  $\mathcal{P}$  plane). The desired workspace is defined by two trajectory segments. This figure shows that effectively the two trajectories lie inside the workspace of a robot whose  $R_1, r_1$  have been taken inside the allowable region. When the allowable region is empty it may be necessary to change the fixed design parameters: the

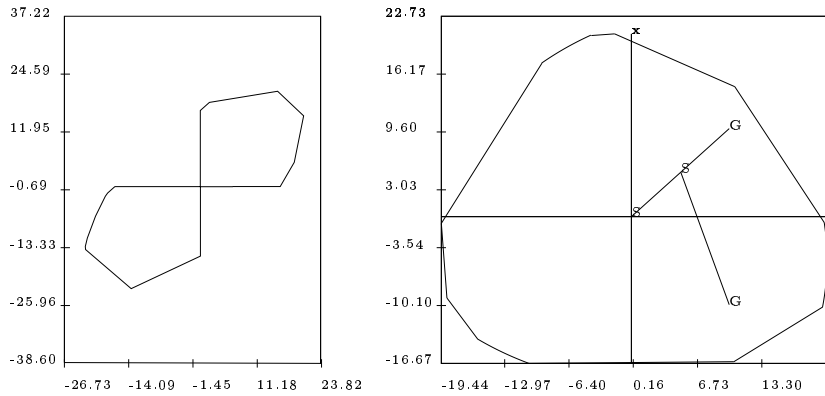


Figure 10: An allowable zone for the whole set of constraints. A robot has been defined by taking the values of  $R_1, r_1$  inside the allowable region. The figure presents the workspace boundary and the trajectories.

angles  $\alpha, \beta$ , the actuator lengths  $\rho_{min}, \rho_{max}$  or the mechanical limits on the joint. For some of these parameters it is possible to determine the minimal values which will lead to the existence of an allowable region (Merlet 1995).

## 4 Extension to different types of desired workspace

As the number of objects used to specify the desired workspace is not limited we may assume that any volume may be approximated by a finite set of segments or points. However it would be interesting to specify directly a set of planar polygons or polyhedra to describe the desired workspace (meaning that the robot workspace should include all the points *inside* the polygon or the polyhedra). In that case the following theorem may be proved:

**Theorem 6** *When the desired workspace is defined as the interior of a polygon (polyhedra) the allowable region for the maximum links length constraint is the intersection of the maximal ellipses computed for all the vertices of the polygon (polyhedra)*

Unfortunately this result does not hold for the minimum links length constraint. Yet the "growing" algorithm may be used with any kind of object although the grown volume is more difficult to compute for polygon and polyhedron. An implementation of the algorithm for these objects is currently under development. The case where the desired workspace is described by a set of spheres as been treated in (Merlet 1995) and the results are quite simple.

As for the mechanical limits constraints on the joint and legs interference constraints the extension of the results obtained for segments workspace to polygons and polyhedra workspaces is the subject of our future work.

## 5 Extension to other types of parallel manipulators

The algorithm described in this paper was illustrated on the Gough-type parallel manipulator. But a similar algorithm may be used for other type of parallel robots. For example consider the 6 DOF INRIA robot (Merlet, Gosselin 1991) (figure 11), which has been used for eye surgery (Grace et al. 1993). In this

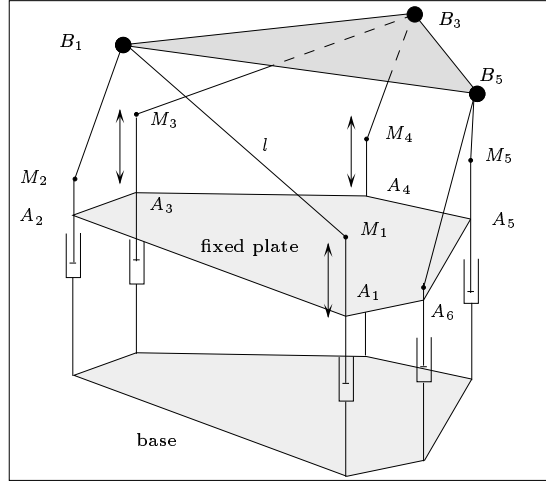


Figure 11: The INRIA robot

type of robot a linear actuator moves center  $M_i$  of the universal joint of the link  $M_iB_i$  along a vertical axis ( $A_i$  is the center of the hole in the fixed plate through which slide the actuators). The moving platform is connected to this link through the ball-and-socket joint of link  $M_iB_i$ . The posture of the moving platform may therefore be controlled by the distance  $\rho_i$  between  $A_i, M_i$  (i.e. the height of  $M_i$  with respect to the fixed plate). We will study now the inverse kinematics of this robot. Let  $l_i$  be the fixed length of link  $M_iB_i$ . We have:

$$\|\mathbf{M}_i\mathbf{B}_i\|^2 = l_i^2 = \|\mathbf{M}_i\mathbf{A}_i + \mathbf{A}_i\mathbf{B}_i\|^2 \quad (23)$$

with  $\mathbf{M}_i\mathbf{A}_i = -\rho_i\mathbf{z}$ . This lead to:

$$\rho_i^2 - 2\rho_i \mathbf{z}\cdot\mathbf{A}_i\mathbf{B}_i + \mathbf{A}_i\mathbf{B}_i^2 - l_i^2 = 0 \quad (24)$$

Note that we may get two solutions to this equation which are either lower or greater than the  $z$  coordinate of  $B_i$ . We will assume here we are interested only in the lowest value,  $B_i$  being always over  $M_i$ . Let us assume now that we have defined the desired workspace as a given posture and that the value of  $\rho_i$  should be in the range  $[\rho_{min}, \rho_{max}]$ . Using the same development as for the Gough-type platform we get that for a fixed value of  $\rho$  equation (24) defines an ellipse in the  $R_1, r_1$  plane. Consider now each point  $Q$  of the  $R_1, r_1$  plane such that:

$$\rho_{max}^2 - 2\rho_{max} \mathbf{z}\cdot\mathbf{A}_i\mathbf{B}_i + \mathbf{A}_i\mathbf{B}_i^2 - l_i^2 \leq 0 \quad (25)$$

i.e. the interior of the maximal ellipsis. Assume now that for a point  $Q$  there exists a value of  $\rho$  such that equation (24) is satisfied. We subtract these two equations to get:

$$\rho_{max}^2 - 2\rho_{max} \mathbf{z}\cdot\mathbf{A}_i\mathbf{B}_i - \rho^2 + 2\rho \mathbf{z}\cdot\mathbf{A}_i\mathbf{B}_i \leq 0 \quad (26)$$

or

$$(\rho_{max} - \rho)(\rho_{max} - 2 \mathbf{z} \cdot \mathbf{A}_i \mathbf{B}_i + \rho) \leq 0 \quad (27)$$

Note that  $\mathbf{z} \cdot \mathbf{A}_i \mathbf{B}_i > 0$ . If we assume that the right term of this inequality is positive, then the value of  $\rho$  corresponds to the solution where  $M_i$  is over  $B_i$ . According to our assumption we may therefore state that this term is negative. Consequently this inequality is satisfied iff  $\rho \leq \rho_{max}$  and the maximal ellipse defines the allowable region with respect to the maximum height constraint. A similar reasoning would show that the minimal ellipse is also the forbidden region with respect to the minimum height for the actuator. Therefore the algorithm developed for the Gough-type platform may be extended to this robot.

## 6 Conclusion

The algorithm presented in this paper enables us to compute the location of the attachment points of all the robots whose workspace contains a desired workspace under the assumption that the minimum and maximum leg lengths are known and that the general direction of the lines on which lie the attachment points are also known.

Various criteria may be used for determining an "optimal" robot, with the numerical algorithm presented, whose search domain has been reduced. Some suitable criteria for an "optimal" robot may be:

1. maximal dexterity over the workspace
2. the least articular forces needed for moving a given load in the specified workspace
3. the least positioning errors for the platform, given the sensor error bounds in leg length measurement
4. the maximal platform velocity, given the bounds on actuator velocities
5. the absence of singularity in the workspace

Finding procedures for efficiently evaluating these issues are still open problems and will constitute to be the subject of future research.

As an example item 3 has been used for designing the robot of the European Synchrotron Radiation Facility (ESRF) presented in figure 12. At the start of this project the workspace was specified as a cube of 2cm side, the required accuracy was 1  $\mu\text{m}$  for a nominal load of 500 kg and the range of the actuators was  $\pm 4\text{cm}$ .

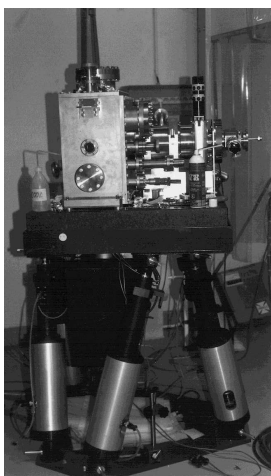


Figure 12: The ESRF robot

The allowable region was determined and a regular grid was defined on the region. At each node of the grid (i.e. for a given robot geometry) the minimal sensor accuracy for obtaining the desired positioning accuracy was determined and a node leading to a sensor accuracy of  $0.87 \mu\text{m}$  was found. During the process it was noted that for another robot whose workspace was satisfactory the sensor accuracy was  $0.0435 \mu\text{m}$ : hence the performances of robots whose workspace includes a given workspace may largely vary and the design has to be carefully studied.

## 7 Appendix: Numerical data of the examples

Table 1: Angles  $\alpha_i, \beta_i$  in degree and minimum and maximum length of the legs (first set)

link	1	2	3	4	5	6
$\alpha_i$	35	145	155	265	275	25
$\beta_i$	85	95	205	215	325	335
$\rho_{min}$	30	30	30	30	30	30
$\rho_{max}$	40	40	40	40	40	40

Table 2: Desired segments

Trajectory 0						Trajectory 1					
0	0	20	0	0	0	5	0	20	0	20	0
10	10	20	0	0	0	-10	10	20	0	20	0

## References

- [Claudinon, Lievre 1985] Claudinon, B. and Lievre, J. 1985 (Oct. 7-12). Test facility for rendez-vous and docking. 36th Congress of the IAF, Stockholm.
- [Gosselin 1988] Gosselin, C. 1988. *Kinematic analysis optimization and programming of parallel robotic manipulators*. Ph.D. Thesis, McGill University, Montréal, Department of Mechanical Engineering.
- [Gosselin 1990] Gosselin, C. 1990. Determination of the workspace of 6-dof parallel manipulators. *ASME J. of Mechanical Design*, 112(3):331–336,
- [Gosselin, Angeles 1988] Gosselin, C. and Angeles, J. 1988. The optimum kinematic design of a planar three-degree-of-freedom parallel manipulator. *J. of Mechanisms, Transmissions and Automation in Design*, 110(1):35–41.
- [Gosselin, Lavoie, Toutant 1992] Gosselin, C. and Lavoie, E. and Toutant, P. 1992 (Sept. 13-16) An efficient algorithm for the graphical representation of the three-dimensional workspace of parallel manipulators. 22nd Biennial Mechanisms Conf., Scottsdale.
- [Grace et al. 1993] Grace, K.W. and others. 1993 (May 2-6). A six degree of freedom micromanipulator for ophthalmic surgery. IEEE Int. Conf. on Robotics and Automation, Atlanta.
- [Liu, Fitzgerald, Lewis 1991] Liu, K. and Fitzgerald, M.K., and Lewis F. 1991 Some issues about modeling of the Stewart platform. 2nd Int. Symp. on Implicit and Robust systems, Warsaw.

- [Liu, Fitzgerald, Lewis 1993] Liu, K. and Fitzgerald, M.K. and Lewis, F. 1993. Kinematic analysis of a Stewart platform manipulator. *IEEE Trans. on Industrial Electronics*, 40(2):282–293.
- [Merlet 1994] Merlet, J-P. 1994. Détermination de l'espace de travail d'un robot parallèle pour une orientation constante. *Mechanism and Machine Theory*, 29(8):1099–1113.
- [Merlet 1995] Merlet, J-P., 1995 (April). Designing a parallel robot for a specific workspace. Research Report 2527, INRIA. <sup>2</sup>
- [Merlet, Gosselin 1991] Merlet, J-P. and Gosselin, C. 1991 Nouvelle architecture pour un manipulateur parallèle à 6 degrés de liberté. *Mechanism and Machine Theory*, 26(1):77–90.
- [Stoughton, Kokkinis 1987] Stoughton, R. and Kokkinis, T. 1987 (June 28). Some properties of a new kinematic structure for robot manipulators. ASME Design Automation Conf., Boston.
- [Trojanov 1995] Trojanov, M., 1995 (April). Note sur le problème de prolégomènes n°10. *Prolégomènes*, (11):3. <sup>3</sup>

---

<sup>2</sup><ftp://zenon.inria.fr/pub/rapports/>

<sup>3</sup><http://www.inria.fr/coprin/equipe/merlet/Prolegomenes/catalogue.html>